Lawrence Berkeley National Laboratory

Title

PALEOCLIMATIC SIGNIFICANCE OF LAKE LEVEL FLUCTUATIONS IN THE LAHONTAN BASIN

Author

Benson, L.V.

Publication Date

1980-08-01

LBL-11265
UC-11 c.2

PALEOCLIMATIC SIGNIFICANCE OF LAKE LEVEL FLUCTUATIONS IN THE LAHONTAN BASIN

L. V. Benson

August 1980

Prepared for the U.S. Department of Energy
under Contract W-7405-ENG-48

LBL-11265

PALEOCLIMATIC SIGNIFICANCE OF LAKE LEVEL FLUCTUATIONS IN THE LAHONTAN BASIN

L. V. Benson

Lawrence Berkeley Laboratory
University of California
Berkeley, CA 94720

This report was prepared with partial support from the U. S. Department of Energy under Contract W-7405-ENG-48.

TABLE OF CONTENTS

	Page
ABSTRACT	iv
INTRODUCTION	1
THE ENERGY BALANCE MODEL	2
TEST OF THE ENERGY BALANCE MODEL	5
PALEO LAKE LEVELS	6
PALEOCLIMATIC SIMULATIONS	7
Evaporation Simulations	7
Discharge Calculations	8
Changes in Climatic Parameters Necessary to Account for Changes in Paleo Lake Levels	9
The Effect of a Glacial Meltdown on the Level of Lake Lahontan	11
The Effect of Ice Cover on the Creation and Maintenance of Lake Lahontan High Stands	12
SUMMARY AND CONCLUSIONS	13
REFERENCES	15
APPENDIX	18
TABLES	
FIGURES	

ABSTRACT

An energy flux balance model has been developed which treats evaporation as a function of air temperature, surface water temperature, precipitable water aloft, the amount, height, and type of sky cover, and the optical air mass.

The model has been used to estimate the mean historical evaporation rate for Pyramid Lake, Nevada, using as input climatic data from the Reno area averaged over the period 1950-1975. Estimated and measured values of the mean annual evaporation rate were found to be in good agreement.

The model was used to simulate changes in the level, the surface area and the volume of paleo Lake Lahontan. In particular, possible climatic states responsible for past high stands (1270 and 1330 m) were investigated. A conservative range of discharge values was used in the calculations. Results of the simulations indicate the fundamental importance of sky cover in the creation and destruction of large lake systems.

INTRODUCTION

During the Quaternary, the Great Basin of the western United States was the site of several large lake systems (Russell, 1885; Gilbert, 1890; Broecker and Orr, 1958; Broecker and Kaufman, 1965; Morrison and Frye, 1965; Mifflin and Wheat, 1977). Various workers have attempted to estimate the type of paleoclimate responsible for the creation and maintenance of these lakes (Russell, 1885; Jones, 1925; Antevs, 1952; Broecker and Orr, 1958; Snyder and Langbein, 1962; Galloway 1970; Reeves, 1973; Brakenridge, 1978) usually postulating a change in the precipitation or evaporation rate as the controlling factor. However, the relative importance of these factors remains controversial.

In order to estimate changes in the evaporation rate, certain workers (e.g., Leopold, 1951) have: 1) correlated the present-day mean temperature of the free atmosphere with the modern snow line, 2) used relict glacial features to determine the location of the snowline in the past, and 3) invoked a correlation between present-day mean monthly evaporation rates and mean monthly air temperatures. This procedure leaves much to be desired since full-glacial cooling has not been shown to occur evenly at both high and low elevations, i.e, Pleistocene lapse rates may have differed from present-day lapse rates. In addition, the extrapolation of present-day air-temperature evaporation-rate correlations to full-glacial periods is risky since it assumes that all other climatic parameters which affect evaporation (humidity, cloud cover, water temperatures, etc.) are correlated with past temperature distributions in the same manner as they are correlated with present-day temperature distributions.

In this study, evaporation across an air-water interface is theoretically formulated in terms of an energy flux balance. This enables calculation of the functional dependence of evaporation on several climatic parameters: air temperature, surface water temperature, precipitable water aloft, the amount, height, and type of cloud cover, and the optical air mass, i.e., the path length traversed by light rays from a celestial body to the observer expressed as a multiple of the path length at zenith. The theoretical model is used to calculate the mean annual evaporation rate for Pyramid Lake, Nevada, a remnant of paleo Lake Lahontan. After testing of the model against measured evaporation rates, it is then used to determine possible climatic states responsible for fluctuations in paleo Lake Lahontan (hereafter referred to as Lake Lahontan).

THE ENERGY BALANCE MODEL

The energy flux balance, in calories per unit are per day, is given by (Harbeck, et al., 1958):

$$Q_s - Q_r + Q_a - Q_{ar} - Q_{bs} + Q_v - Q_e - Q_h - Q_w = \Delta Q_\nu \quad (1)$$

Q_s is the solar radiation flux incident to the water surface and can be calculated with the following relation

$$Q_s = Q^* \tau_{AB} \tau_{DA} \tau_{WS} \tau_{WA}. \quad (2)$$

In Eqn. 2, Q^* is the mean daily solar radiation flux incident on the upper atmosphere at the latitude of interest. τ_{AB}, τ_{DA}, τ_{WS}, and τ_{WA} are atmospheric transmission coefficients due respectively to cloud albedo, dry air, water vapor scattering and water vapor adsorption.

Q_r, the flux of solar radiation reflected from the water surface, is given by

$$Q_r = R_s Q_s \quad (3)$$

where R_s is the surface reflectivity.

The flux of incoming long-wave atmospheric radiation, Q_a, is related to the temperature, T_a, and vapor pressure, e_a, of the air measured at a standard distance above the surface, i.e.,

$$Q_a = \delta T_a^4 (a + be_a) \tag{4}$$

where a, b and δ are constants.

Q_{ar}, the amount of reflected long-wave radiation, is given by

$$Q_{ar} = R_a Q_a \tag{5}$$

where R_a is the long-wave reflectivity of the water surface.

The flux of long-wave radiation emitted by the water, Q_{bs}, is given by

$$Q_{bs} = \delta T_o^4 \bar{e} \tag{6}$$

where T_o is the water surface temperature in degrees Kelvin and $\bar{e}$ is the emissivity of water.

Q_v, the net energy flux advected into the water body, can be calculated by summarizing the heat contributions from all advective sources, i.e.,

$$Q_v = \rho V_i'(\bar{T}_i - T_b)c \tag{7}$$

where V_i is the volume input to the water body from the i^{th} source, $\bar{T}_i$ is the mean temperature of the i^{th} source, and ρ and c are, respectively, the density and specific heats of water.

Q_e, the energy flux due to evaporation, is related to the density of water being evaporated, ρ_e, the evaporation rate, E, and the latent heat of vaporization, L, by

$$Q_e = \rho_e EL. \tag{8}$$

Q_h, the energy flux conducted from the water as sensible heat (enthalpy), is related to the evaporation flux through the Bowen ratio, R, by

$$Q_h = RQ_e. \tag{9}$$

Q_w, the energy flux advected by evaporating water, is given by

$$Q_w = \rho_e cE(T_o - T_b). \tag{10}$$

The parameters given in Eqn. 10 have all been previously defined except T_b which is an arbitrary base temperature, usually taken to be 0°K.

Q_ν, the amount of stored energy can be calculated using the following relation

$$Q_\nu = \sum_{i=1}^{j} \rho c(\bar{T}_i - T_b)\, \Delta X_i \bar{A}_i \tag{11}$$

where $\bar{T}_i$ is the mean temperature of the i^{th} layer having thickness ΔX_i and $\bar{A}_i$ is the mean area of the i^{th} layer.

Equations (1) - (11) together with the expression for the Bowen ratio, i.e.,

$$R = \gamma \frac{(T_o - T_a)P}{(e_o - e_a)10^3} \tag{12}$$

can be solved in terms of the evaporation rate, E, giving

$$E = [(1 - R_s)(Q^* \tau_{AB}\tau_{DA}\tau_{WS}\tau_{WA}) + (1 - R_a)(\delta T_a^4 \{a + be_a\})$$

$$- \delta T_o^4 \bar{e} - \Delta \sum_{i=1}^{j} \rho c(\bar{T}_i - T_b)\Delta X_i \bar{A}_i + \rho c(\bar{T}_i - T_b)V_i]/$$

$$[\rho_e(1 + \gamma \frac{\{T_o - T_a\}P}{\{e_o - e_a\}10^3}) + c(T_o - T_b)]. \tag{13}$$

The parameters T_a, T_o, $\bar{T}_i$, T_b, ΔX_i, $\bar{A}_i$, V_i, P, e_o, and e_a are obtained by measurement. The remaining parameters are calculated from various empirical relationships (see Appendix 1).

TEST OF THE ENERGY BALANCE MODEL

In order to test the energy flux balance model, calculations of mean monthly evaporation rates from Pyramid Lake, Nevada, were conducted and the results compared with data from Harding (1965). Mean monthly meteorological data for the 25 year period 1950-1975 (Climatological Data, National Summary) and mean monthly surface temperatures from Pyramid Lake for the period 1976-1977 (Sigler et al. 1978) were used in the calculations. Data for the type of cloud cover and change in heat storage (ΔQ_ν) were unavailable. Therefore, the assumption was made that the mean annual amounts of heat gained and lost by Pyramid Lake were equivalent, i.e.,

$$\sum_{i=1}^{12} \Delta Q_{\nu_i} = 0 \qquad (14)$$

and cloud cover type was treated as an adjustable parameter.

The input and results for a sample calculation are shown in Table 1. Measured evaporation rates for Pyramid Lake are given in Table 2. In Table 3 are shown the results (mean annual evaporation rates) of four calculations in which the relative amounts of low and high level clouds were varied. Note that low and high level clouds were assigned heights of one and six km, respectively. The results of two calculations are graphically displayed, together with the data of Harding (1965), in Figure 1.

The set of calculated annual evaporation rates are in close agreement with the measured values (Tables 2 and 3); however, the calculated mean monthly distributions are not coincident with the measured mean monthly distribution (Fig. 1). This is probably a result of not accounting for month-to-month changes in heat storage. Note also that the calculations are not particularly sensitive to the type of sky cover. This is due to the fact that during the period of interest a high percentage of the total annual evaporation occured in months characterized by low percentages of sky cover (Table 1).

In general, the energy balance model yields satisfactory results when applied to the calculation of mean annual historical evaporation rates. In the following section the model is used to deduce changes in certain climatic parameters which may have led to fluctuations in the level of Lake Lahontan.

PALEO LAKE LEVELS

Fluctuations in the level of Lake Lahontan have been documented by a variety of researchers. Broecker and his co-workers (Broecker and Orr, 1958; Broecker and Walton, 1959; Broecker and Kaufman, 1965) were the first to attempt a determination of the absolute chronology of Lake Lahontan. Certain inconsistencies in Broecker's radiocarbon determinations led to a redetermination of the chronology (Benson, 1978). An additional 44 carbon-bearing samples have been age-dated as part of the present study (Table 4). The new data are substantially in accord with the author's previous findings (Benson, 1978) and are correlative with recent studies of Searles Lake (Smith, 1968; Peng et al., 1978) and Lake Bonneville (Scott, 1980).

The main features of the Lahontan chronology, depicted in Figure 2, are (1) extreme high stands (1330 m above sea level) 13,500 to 11,000 and 25,000 to 22,000 B.P., (2) a moderate high stand (1260 m above sea level) 20,000 to 15,000 B.P. (3) a low stand of unknown elevation prior to 25,000 B.P. (4) an extremely low stand from 9000 to 5000 B.P., and (5) an overall increase in the size of Walker and Pyramid Lakes during the past 5000 years, until the late 19th century.

With regard to the rate of lake-level change, data from Pyramid Basin indicate that the lake rose 100 m in either a 10,000 or a 2000 year period (trajectories 3 and 4 of Fig. 2). This represents a rate of increase of .01 to .05 m yr^{-1}. The rate of lake-level decline which occurred at 11,000 B.P. was on the order of .08 to .15 m yr^{-1} (trajectories 1 and 2 of Fig. 2).

Hydrographic characteristics of Lake Lahontan for various key times in the past are given in Table 5. Some of the data used to estimate these parameters were obtained by planimetering each of the nine Lahontan subbasins (Fig. 3). The hydrographic parameters for the 1180 m lake level were obtained from Russell (1885). The parameters for the 1230 and 1270 m lake levels were estimated assuming that all lakes, even though physically unconnected, stood at the same level as the Pyramid Basin lake.

PALEOCLIMATIC SIMULATIONS

Changes in lake level, volume, and surface area occur in response to changes in the hydrologic balance, i.e., changes in the rate of fluid input and/or the rate of evaporation.

Evaporation Simulations

In Figure 4, air temperature, precipitable water aloft and sky cover distributions used in the simulations are compared seasonally with mean historic values. Two types of simulated distributions were utilized. In one case an absolute change in the value of a parameter was added to each of the monthly values. In the second case it was assumed that there was a graduated change in the parameter for each month, with the maximum change in July and no change in January. For example, the mean temperature of each month was decreased by a constant percentage of the difference between the temperature of that month and the January temperature. "Ice-age" values for air temperature and precipitable water aloft were chosen in light of Gates' (1972) global climatic synthesis of the 18,000 B.P. climate. Changes in sky cover were arbitrarily chosen.

Some of the results of the simulations are shown in Figure 5. The results of calculations in which precipitable water aloft was varied from 20 to 40 percent differed by less than two percent and therefore have not been shown. It is apparent from the data of Figure 5, that July-scaled temperature reductions of 10-15° K and sky cover increases of 10-20 percent (absolute) serve to reduce the annual evaporation rate by 45-60 percent (curves 1-4). Changes in sky cover, uniformly distributed over the year, cause a further reduction in the evaporation rate (compare curves 1 and 7); while uniformly distributed changes in both sky cover and temperature (10 percent and 10° K, respectively) serve to reduce the evaporation rate to less than 25 percent of its present value (see curve 9 of Fig. 5).

Discharge Calculations

Historic mean annual discharge to the Lahontan Basin from the four principal river systems depicted in Figure 3 have been calculated using an evaporation rate of 1.25 m yr^{-1} (Harding, 1965) together with the total surface area of perennial lakes observed by Russell (1885). The results of the calculations are given in Table 6.

The amount of discharge to the Lahontan Basin during a full-glacial period is a matter of controversy. The only study that has dealt even semi-quantitatively with past changes in Sierran precipitation is that of Curry (1969). Curry estimated that in order to create and maintain the Sierran glacier which existed during the Wisconsin maxima, the mean snowfall would have had to be 2.5 times the present mean snowfall, assuming that summer cloud cover, ground albedo, and temperature during the glacial maxima were the same as those for the period 1930 to 1960. With cool, cloudy summers such as those of 1895 and 1907, 1.2 times the present mean winter snowfall would have been sufficient.

The functional relationship that existed between increased snowfall and discharge to the Lahonton basin during the Wisconsin is not known. One approach is to assume that a linear 1:1 relationship existed such that discharge ranged from 2.2 to 4.5 km^3 yr^{-1}. This estimate of discharge may be somewhat conservative for glacial periods. However, for the purpose of further discussion, we have used this estimate recognizing the deficiencies of the assumption used in its calculation.

Changes in Climatic Parameters Necessary to Account for Changes in Paleo Lake Levels

Given the hydrographic data of Table 5, evaporation rates of .10 and .20 m yr^{-1} are necessary to maintain a steady state 1330 m high stand with input fluxes of 2.2 or 4.5 km^3 yr^{-1}, respectively. To maintain a 1270 m high stand, evaporation rates of .14 and .29 m yr^{-1} are required. Model calculations show that these evaporation rates can be achieved with absolute monthly sky cover increases of 10 percent, mean air temperature decreases of no less than 10°K, and heap cloud percentages in excess of 10 percent (Fig. 5). Note, for example, curve 9 of Figure 5 where the present-day mean monthly temperature distribution has been reduced by 10°K. In this case, a change in the amount of heap clouds from 10 to 30 percent caused a decrease in the evaporation rate from .30 to .15 m yr^{-1}.

Documented rates of lake level change impose additional constraints on the permissible range of evaporation rates. Two periods of rapid lake level change are of particular interest (trajectories 4 and 2 of Fig. 2). Trajectory 4 represents a rise in lake level of 100 m which occurred within a 2000 year period. Trajectory 2 represents a fall of lake level of 150 m in approximately 1000 yr.

In order to calculate the response in lake level to changes in climatic parameters, it was assumed that climatic changes occurred instantaneously at 15,000 B.P. to values sufficient to maintain the 13,000 B.P. lake level and at 11,000 B.P. to historic values.

The volume of water lost to evaporation, V_E, during the 2000 yr period represented by trajectory 4 is equal to the product of the mean evaporation rate, the mean surface area, and the time over which the process took place. Given evaporation rates of .20 and .10 m yr^{-1},

$$V_E(.2) = (2.0 \times 10^{-4} \frac{km}{yr})(1.6 \times 10^4 \ km^2)(2 \times 10^3 \ yr) = 6.4 \times 10^3 \ km^3 \quad (15)$$

and

$$V_E(.1) = (1.0 \times 10^{-4} \frac{km}{yr})(1.6 \times 10^4 \ km^2)(2 \times 10^3 \ yr) = 3.2 \times 10^3 \ km^3. \quad (16)$$

The volume of water input to the lake V_D during the 2000 yr period is given by the discharge rate multiplied by the duration of the discharge process. For discharge rates of 4.5 and 2.2 km^3 yr^{-1},

$$V_D(4.5) = (4.5 \frac{km^3}{yr})(2 \times 10^3 \ yr) = 9.0 \times 10^3 \ km^3 \quad (17)$$

and

$$V_D(2.2) = (2.2 \frac{km^3}{yr})(2 \times 10^3 \ yr) = 4.4 \times 10^3 \ km^3 . \quad (18)$$

The net volume change is equivalent to the amount discharged minus the amount evaporated, i.e.,

$$\Delta V_1 = V_D(4.5) - V_E(.2) = 2.6 \times 10^3 \ km^3 \quad (19)$$

and

$$\Delta V_2 = V_D(2.2) - V_E(.1) = 1.2 \times 10^3 \ km^3 . \quad (20)$$

In order for the lake to rise from 1230 to 1330 m, the net volume change must equal 1660 km^3. Therefore, an evaporation rate of 0.20 m yr^{-1} combined with a discharge rate of 4.5 km^3 yr^{-1} is sufficient to account for the apparent change in lake level; however, an evaporation rate of 0.10 m yr^{-1} combined with a discharge rate of 2.2 km^3 yr^{-1} is not sufficient.

If we assume that historic evaporation and discharge rates were instantaneously achieved at 11,000 B.P., then over 1000 yr the potential volume of evaporated water is

$$V_E(1.2) = (1.2 \times 10^{-3} \frac{km}{yr})(1.2 \times 10^4 \ km^2)(1 \times 10^3 \ yr) = 1.4 \times 10^4 \ km^3 \quad (21)$$

where the mean surface area (1.2 x 10^4 km^2) was set equal to one-half the sum of the 1180 and 1330 m values. The volume discharged to the lake during the same period of time was

$$V_D(1.8) = (1.8 \frac{km^3}{yr})(1 \times 10^3 \ yr) = 1.8 \times 10^3 \ km^3. \quad (22)$$

Thus, the net potential volume change was

$$\Delta V_3 = V_D(1.8) - V_E(1.2) = -1.2 \times 10^4 \ km^3. \quad (23)$$

Since the actual difference in volume between the 1330 and 1180 m high stands is less than 2.1 x 10^2 km^3 (Table 5), it is clear that Lake Lahontan could have fallen 150 m in less than 1000 yr given an instantaneous change in climate at 11,000 B.P. to present-day values.

The Effect of a Glacial Meltdown on the Level of Lake Lahontan

It is reasonable to assume that the Sierran glacier began to melt during or shortly after the 1330 m high stand. If so, what was the effect of the increased discharge on lake level? And, in particular, was the 1330 m high stand prolonged for a significant period of time as a result of the increased volume of meltwater discharged to the Lahontan Basin?

The total amount of glacial ice stored in the eastern Sierran catchment area was less than 750 km^3. Assuming as before, that the evaporation rate changed instantaneously to 1.2 m yr^{-1}, the annual volume of water evaporated from the 1330 m surface would have been

$$\frac{\Delta V}{\Delta t} = (1.2 \times 10^{-3} \frac{km}{yr}) (2.2 \times 10^{4} km^{2}) = 26 \frac{km^{3}}{yr} . \qquad (24)$$

Therefore, given the previous assumptions, a melting of the Sierran glacier could have prolonged the 1330 m high stand for no more than 30 years. This could not have caused a significant time lag between climatic change and lake level response.

The Effect of Ice Cover on the Creation and Maintenance of Lake Lahontan High Stands

In estimating the change in climate necessary for the creation and maintenance of Lake Lahontan, the effect of seasonal ice cover was not given consideration. The annual heat budget of a lake is of course affected by ice cover. In winter, ice cover acts as a store of latent heat and modifies energy exchanges between the lake and the atmosphere. In spring, additional heat is required to raise the temperature of the ice cover to its melting point, to effect its change of state to the liquid and also to heat the liquid. A quantitative estimate of the effect of seasonal ice cover on the evaporation rate is beyond the scope of this paper (for a discussion of this topic see Adams and Lasenby, 1978). However, it is clear that ice cover causes a reduction in the evaporation rate. If the surface of Lake Lahontan was ice covered, it follows that the amount of climatic change necessary for the creation and maintenance of high stands has been overestimated in the previous calculations.

SUMMARY AND CONCLUSIONS

An energy flux balance model has been developed, tested, and applied to the calculation of evaporation from an open body of water. The model treats evaporation as a function of air temperature, surface water temperature, precipitable water aloft, the amount, height, and type of cloud cover, and the optical air mass.

The model has been used to simulate changes in level, surface area and volume of Lake Lahontan. Conservative estimates of discharge were used in the calculations. Simulations of paleo high stands of Lake Lahontan were achieved by increasing historical values of sky cover by 10 percent (absolute), by reducing the mean air temperature by at least 10°K, and by assuming that the percentage of heap clouds exceeded 10 percent. Such calculations resulted in evaporation rates which are an order of magnitude smaller than present-day values.

The rate of change of paleo lake levels places an additional constraint on paired values of discharge and evaporation. Calculations assuming instantaneous changes of climate show that evaporation rates in the range .13 to .20 m yr^{-1} are sufficient to account for the most rapid, documented rise in lake level. Instantaneous changes of evaporation and discharge rates to their historic values are also more than sufficient to account for the documented 150 m drop in lake level at 11,000 B.P.

Results of calculations using the energy balance approach point to the overriding influence of sky cover on changes in the hydrologic balance of closed basin systems. Precipitable water aloft, precipitation, and air and surface water temperatures are all functions of the amount and type of sky cover. Therefore, cloud cover rather than evaporation or precipitation should be considered the master variable which governs fluctuations of paleo lake systems.

In conclusion, it should be noted that the energy flux balance model has hidden within its parameter set the effect of such dynamic variables as wind velocity. The application of this model to past times is appropriate only to the extent that the correlations between empirical terms in the energy flux balance equation and the set of dynamic processes remain the same.

REFERENCES

Adams, W. P., and Lasenby, D. C. (1978). The role of ice and snow in lake heat budgets. Limnol. Oceanogr. 23, 1025-1028.

Antevs, E., (1952). Cenozoic climates of the Great Basin. Geol. Res. 40, 94-108.

Benson, L. V. (1978). Fluctuation in the level of pluvial Lake Lahontan during the last 40,000 years. Quaternary Research 9, 300-318.

Brakenridge, G. R. (1978). Evidence for a cold, dry full-glacial climate in the American southwest. Quaternary Research 9, 22-40.

Broecker, W. S., and Kaufman, A. (1965). Radiocarbon chronology of Lake Lahontan and Lake Bonneville II. Great Basin. Geological Society of America Bulletin 76, 537-566.

Broecker, W. S., and Orr, P. C. (1958). Radiocarbon chronology of Lake Lahontan and Lake Bonneville. Geological Society of America Bulletin 69, 1009-1032.

Broecker, W. S., and Walton, A. (1959). The geochemistry of C^{14} in fresh-water systems. Geochmica et Cosmochimica Acta 16, 15-38.

Climatological Data, National Summary (1950-1974). National Oceanographic and Atmospheric Administration, Environmental Data Service, National Climatic Center, Federal Building, Asheville, N.C.

Curry, R. R. (1969). Holocene climatic glacial history of the central Sierra Nevada. Geological Society of America Special Paper 123, 1-48.

Davies, J. A., Schertzer, W., and Nunez, M. (1975). Estimating global solar radiation. Boundary-Layer Meteorology 9, 33-52.

Galloway, R. W. (1970). The full-glacial climate in the southwestern United States. Annals of the Association of American Geographers 60, 245-256.

Gates, W. L. (1976). Modeling the ice-age climate. Science 191, 1138-1144.

Gilbert, G. K. (1890). Lake Bonneville. United States Geological Survey Monograph 1, 375p.

Harbeck, G. E., Jr., Dennis, P. E., Kannon, F. W., Anderson, L. J., Marciano, J. J., and Kohlen, M. A. (1954). Water-loss investigations: Lake Hefner studies, Technical Report, United States Geological Survey Professional Paper 269, 157 pp.

Harbeck, G. E., Jr., Kohler, M. A., Koberg, G. E., and others (1958). Water-loss investigations: Lake Mead Studies, United States Geological Survey Professional Paper 298, 100pp.

Harding, S. T. (1965). Recent variations in the water supply of the western Great Basin. University of California Archive Series Report 16, 226pp.

Jones, J. C. (1925). The geologic history of Lake Lahontan. In Quaternary Climates, Carn. Inst. Wash. Publ., 352, 1-49.

Kasten, F. (1966). A new table and approximation formula for the relative optical air mass. Archiv fur meteorologie, geophysik, und bioklimatologie Serie B. Allgemeine und biologische klimatologie, band 14, 2. heft, 206-223.

Leopold, L. B. (1951). Pleistocene climate in New Mexico. American Journal of Science 249, 152-168.

List, R. J. (1951). Smithsonian Meteorologial Tables, 6th edition. Publication 4014 of the Smithsonian Institution Washington, D.C., 527 pp.

Mifflin, M., and Wheat, M. (1977). Pluvial lakes of Nevada and estimated full pluvial climates. Publication of the Water Resources Center of the Desert Research Institute, Reno, Nevada, 77pp.

Morrison, R. B., and Frye, J. C. (1965). Correlation of the Middle and Late Quaternary successions of the Lake Lahontan, Lake Bonneville, Rocky Mountain (Wasatch Range)., Southern Great Plains, and Eastern Midwest Areas. Report 9 of th Nevada Bureau of Mines, 45pp.

Peng, T.-H., Goddard, J. G., and Broecker, W. S. (1978). A direct comparison of ^{14}C and ^{230}Th ages at Searles Lake, California. Quaternary Research 9, 319-329.

Reeves, C. C., Jr. (1973). The full-glacial climate of the southern high plains,. West Texas. Journal of Geology 81, 693-704.

Reitan, C. H. (1963). Surface dew point and water vapor aloft. Journal of Applied Meteorology 2, 766-779.

Russell, I. C. (1885). Geological history of Lake Lahontan, United States Geological Survey Monograph 11, 288p.

Scott, W. E. (1980). New interpretations of the late Quaternary history of Lake Bonneville, western United States. Abstracts of the 6th biennial meeting of the Am. Quaternary Assoc., 168-169.

Sellers, W. D. (1965). Physical Climatology. University of Chicago Press, Chicago, 272pp.

Sigler, W. F. (1978). Pyramid Lake Ecological Study. Pub. by W. F. Sigler, Associates and Co., Logan, Utah, 545 pp.

Snyder, C. T., and Langbein, W. B. (1962). The Pleistocene Lake in Spring Valley, Nevada, and its paleoclimatic implications. J. Geophys. Res., 67, 2385-2394.

Smith, G. I. (1968). Late-Quaternary geologic and climatic history of Searles Lake. Southeastern California. In "Means of Correlation of Quaternary Successions. Vol. 8: Proceedings VII Congress International Association for Quaternary Research" (R. B. Morrison and H. E. Wright, Jr., Eds.) p. 293. University of Utah Press, Salt Lake City, Utah.

Wahrhaftig, C., and Birman, J. H. (1956). The Quaternary of the Pacific Mountain system in California. In "The Quaternary of the United States" (Wright and Frey, Eds.), pp. 299-339. Princeton University Press, Princeton, N. J.

Weast, R. C. (1976). Handbook of Chemistry and Physics, 57th edition, CRS Press, Cleveland, Ohio.

APPENDIX. Parameters and Relationships Used in Calculating the Evaporation Rate.

ρ_e = 1.00 g cm^{-3}

ρ = 1.00 g cm^{-3}

L = $L(T_o)$ cal g^{-1}. Data from List (1951).

c = 1.00 cal $g^{-1}{}^\circ K^{-1}$

T_b = 0°K

$$e_o = 1.333 \times 10^{\left[\frac{5.409(T_a - 373.15) - 0.508 \times 10^{-8}\{(6.382 - T_a)^4 - (265)^4\}}{T_a} + 2.881\right]} \text{mb}$$

γ = 0.61 (dimensionless)

δ = 11.71 x 10^{-8} ly day^{-1} $°K^{-4}$ (Stefan's constant)

R_s ≅ 0.07 (dimensionless)

R_a ≅ 0.0301 (dimensionless)

$\bar{e}$ = -.970 ± 0.005 (dimensionless)

a = 0.740 + 0.025 χexp(-0.1916h)

b = 0.00490 - 0.00054 χexp(-0.1969h)

χ = fraction of sky cover (dimensionless) was obtained from observations or used as an adjustable parameter.

h = cloud height in km (dimensionless) was obtained from observation (see text).

Q^*(JAN) = 385 ly day^{-1}
(FEB) = 500
(MAR) = 675
(APR) = 835
(MAY) = 950
(JUN) = 1050
(JUL) = 990
(AUG) = 890
(SEP) = 745
(OCT) = 565
(NOV) = 420
(DEC) 355

τ_{DA} = 0.972 - 0.08262 M + 0.00933M^2 - 0.00095M^3 + 0.0000437M^4 (dimensionless)

τ_{WS} = 1 - 0.0225 WM (dimensionless)

τ_{WA} = $1 - 0.077(WM)^{0.30}$ (dimensionless)

W = $\exp(0.1102 + 0.06138\ T_{DP})$ cm. W is the amount of precipitable water aloft and T_{DP} is the dewpoint temperature, a measured parameter.

M(JAN) = 2.99 (dimensionless)
(FEB) = 2.57
(MAR) = 2.11
(APR) = 1.90
(MAY) = 1.81
(JUN) = 1.70
(JUL) = 1.78
(AUG) = 1.85
(SEP) = 2.01
(OCT) = 2.36
(NOV) = 2.83
(DEC) = 3.16

The optical air mass, M, is a function of the zenith angle, z. Values of M = M(z) were taken from Kasten (1966). The zenith angle itself was calculated using the expression

$$\cos(z) = Q^*/S(\bar{d}/d)^2 60\bar{t}.$$

$\underline{S}$ = 2.0 ly min^{-1} (the solar constant)
$\underline{t}$ = hrs of daylight
$\bar{d}/d$ (the ratio of the mean distance of the earth from the sun to the instantaneous distance) = 1.00 ± 0.03 (dimensionless)

τ_{AB} = $1 - (A_{HL}f_{HL}\chi + A_{ML}f_{ML}\chi + A_{LL}f_{LL}\chi)$ (dimensionless)

A_{HL} the albedo of high level clouds = .21
A_{ML} the albedo of high level clouds = .48
A_{LL} the albedo of low level clouds = .70

f_{HL}, f_{ML} and f_{LL} the fractions of respectively, high level, medium level and low level clouds, were used as adjustable parameters in all simulations.

Data sources not previously mentioned are: Davies, et al. (1975), Harbeck et al. (1954 and 1958), Sellers (1965), Reitan (1963) and Weast (1976).

TABLES

TABLE 1

EVAPORATION SIMULATIONS USING HISTORIC DATA (1950 - 1975)

10 PERCENT HEAP CLOUDS

	JAN	FEB	MAR	APR	MAY	JUN	JUL	AUG	SEP	OCT	NOV	DEC
T_a	273.0	276.4	278.2	281.2	285.8	290.0	294.2	293.0	288.6	283.6	277.6	273.6
T_o	279.7	279.7	279.7	282.2	285.2	289.7	294.2	294.2	293.2	290.7	287.2	283.2
HUMID	.63	.55	.48	.43	.42	.39	.34	.35	.39	.47	.56	.63
W	.75	.82	.81	.88	1.11	1.33	1.50	1.41	1.23	1.09	.89	.78
X	.65	.61	.58	.55	.48	.35	.22	.21	.23	.29	.57	.63
P	866.	865	863.	862.	863.	863.	865.	864.	864.	865.	866.	866.
M	2.99	2.57	2.11	1.90	1.81	1.70	1.78	1.84	2.01	2.36	2.83	3.16
Q^*	385.	500.	675.	835.	950.	1050.	990.	890.	745.	565.	420.	355.
L	593.7	593.7	593.7	592.2	590.5	588.0	585.4	585.4	586.0	587.4	589.4	591.7
τ_{DA}	.79	.81	.83	.84	.85	.85	.85	.85	.84	.82	.79	.78
τ_{WS}	.95	.95	.96	.96	.95	.95	.94	.94	.94	.94	.94	.94
τ_{WA}	.90	.90	.91	.91	.91	.90	.90	.90	.90	.90	.90	.90
τ_{AB}	.832	.842	.850	.858	.876	.909	.943	.946	.940	.899	.852	.837
Q_s	216.	293.	417.	529.	610.	698.	668.	602.	498.	351.	241.	196.
Q_r	15.	20.	29.	37.	43.	49.	47.	42.	35.	25.	17.	14.
Q_{bs}	695.	695.	695.	720.	751.	800.	851.	851.	839.	811.	773.	731.
Q_a	496.	523.	536.	561.	604.	645.	688.	673.	629.	584.	533.	501.
Q_{ar}	15.	16.	16.	17.	18.	19.	21.	20.	19.	18.	16.	15.

MEAN MONTHLY EVAPORATION (cm)

JAN	FEB	MAR	APR	MAY	JUN	JUL	AUG	SEP	OCT	NOV	DEC
-.40+	3.14	9.27	14.62	21.17	24.24	22.02	17.29	9.90	3.12	-1.04+	-1.84+

MEAN ANNUAL EVAPORATION = 1.215 m yr^{-1}

+Minus sign indicates condensation onto lake surface.

TABLE 2

MEASURED MEAN MONTHLY EVAPORATION RATES (CM) FOR PYRAMID LAKE.

DATA FROM HARDING (1965).

Evaporation from Pyramid Lake (1932-1947)

Monthly Means ($\bar{x}$) and Standard Deviations (σ)

	JAN	FEB	MAR	APR	MAY	JUN	JUL	AUG	SEP	OCT	NOV	DEC	*Σ
$\bar{x}$	7.6	7.4	6.9	6.4	6.9	9.8	11.9	15.5	16.5	14.3	11.6	9.8	1.25
σ	2.6	2.3	2.4	4.1	2.9	2.2	3.1	2.9	4.4	3.6	3.3	3.6	

*Σ = Mean annual evaporation in m yr^{-1}.

TABLE 3

ESTIMATES OF MEAN HISTORIC EVAPORATION

PARAMETER SPECIFICATION	ANNUAL EVAPORATION RATE ($m\ yr^{-1}$)
HISTORIC DATA (1950-75)	
0% low clouds, 100% high clouds	1.26
10% " 90% "	1.22
20% " 80% "	1.17
30% " 70% "	1.12

TABLE 4

ELEVATIONS AND RADIOCARBON AGES OF UNCONTAMINATED CARBON-BEARING MATERIALS FROM THE LAHONTAN BASIN

Walker Lake: Northeast Shore (Site 9; Benson, 1978)

Sample	Elevation (m)	Age (yr B.P.)
WL-1T	1312	25,280 ± 750
2T	1324	12,340 ± 160
3T	1327	12,275 ± 160

Walker Lake: Western Shore (Site 10; Benson, 1978)

Sample	Elevation (m)	Age (yr B.P.)
WL-4T	1211	2185 ± 80
5T	1216	1335 ± 75
6T	1222	1720 ± 80
7T	1229	1205 ± 75
9T	1244	4445 ± 95
10T	1252	2970 ± 85
14T	1318	12,240 ± 160
15T	1327	11,850 ± 160

Walker Lake: Northwestern Shore (Site 11; Benson, 1978)

Sample	Elevation (m)	Age (yr B.P.)
WL-16B	1332	11,075 ± 160
17T	1328	21,480 ± 175
101T	~1330	13,340 ± 190
102T	~1330	13,300 ± 190
103T	~1330	13,300 ± 190

Adrian Pass: Between Walker and Carson Basins (Site 12; Benson, 1978)

Sample	Elevation (m)	Age (yr B.P.)
AD-2T	~1295	11,880 ± 170
3T	~1302	12,275 ± 175

TABLE 4 (continued)

Pyramid Lake: North shore (Sites 2 and 3; Benson, 1978)

Sample	Elevation (m)	Age (yr B.P.)
PL-15T	1230	15,140 ± 250
16T	1238	21,370 ± 420
17T	1260	18,580 ± 310
18T	1267	16,510 ± 250
20T	1311	13,550 ± 195
21T	1325	12,610 ± 180
22G	1260	19,620 ± 360
23T	1260	19,620 ± 350
44BT	1260	20,180 ± 350
44CT	1260	19,910 ± 350
44DT	1260	19,525 ± 350

Pyramid Lake: Southwest Shore (Site 5; Benson, 1978)

Sample	Elevation (m)	Age (yr B.P.)
PL-40B	1170	875 ± 74

Pyramid Lake: Southeast Shore (Marble Bluff)

Sample	Elevation (m)	Age (yr B.P.)
PL-108T	1235	19,990 ± 380
109T	1242	19,820 ± 340
110T	1303	17,300 ± 200
112T	1303	12,890 ± 190
113T	1326	12,770 ± 190

Pipeline Canyon: 25 km South of Pyramid Lake (Site 6; Benson, 1978)

Sample	Elevation (m)	Age (yr B.P.)
PL-41T	~1311	13,430 ± 195
41G	~1311	13,260 ± 200
43T	~1328	11,430 ± 160
100T	~1312	13,820 ± 200
101T	~1312	13,130 ± 190
102T	~1312	12,570 ± 190
103T	~1321	12,540 ± 190
104T	~1321	12,850 ± 190
105T	~1324	13,050 ± 190

Samples ending in B, T and G indicate respectively: Beach rock, algal tufa, and gastropods. Approximately 50% of each sample was acid leached prior to radiocarbon dating.

TABLE 5

HYDROGRAPHIC CHARACTERISTICS OF LAKE LAHONTAN FOR VARIOUS KEY TIMES IN THE PAST. ALSO GIVEN ARE COMBINATIONS OF THE EVAPORATION RATE AND INPUT FLUX (DISCHARGE) NECESSARY TO MAINTAIN THE GIVEN SURFACE AREA.

Surface Area = 1550 km^2

Elevation = 1180 m
Date = 10,000 B.P., 1845 A.D.

Evap. Rate ($m\ yr^{-1}$)	Input Flux ($km^3\ yr^{-1}$)
1.25	1.94
0.75	1.16
0.25	0.39

Surface Area = 15,530 km^2
Volume = 920 km^3
Elevation = 1270 m
Date = 20,000 - 15,000 B.P.

Evap. Rate ($m\ yr^{-1}$)	Input Flux ($km^3\ yr^{-1}$)
1.25	19.4
0.75	11.6
0.25	3.89

Surface Area = 9690 km^2
Volume = 356 km^3
Elevation = 1230 m
Date = 15,000 B.P.

Evap. Rate ($m\ yr^{-1}$)	Input Flux ($km^3\ yr^{-1}$)
1.25	12.11
0.75	7.27
0.25	2.43

Surface Area = 22,260 km^2
Volume = 2018 km^3
Elevation = 1330 m
Date = 13,500 - 11,000 B.P.

Evap. Rate ($m\ yr^{-1}$)	Input Flux ($km^3\ yr^{-1}$)
1.25	27.3
0.75	16.7
0.25	5.57

TABLE 6

MEAN ANNUAL FLUID INPUTS TO THE LAHONTAN BASIN

RIVER	INPUT FLUX ($km^3\ yr^{-1}$)
Humboldt	0.3
Truckee	0.7
Carson	0.4
Walker	0.4

F I G U R E S

FIGURE CAPTIONS

1. Comparison of measured and calculated mean monthly evaporation rates. E refers to total mean annual evaporation given in meters.

2. Elevation of Lake Lahontan constructed from Pyramid and Walker Basin data. Size of sample is equivalent to counting error. Lines labeled (1), (2), (3), and (4) represent possible trajectories for fluctuations in lake level. Note that the bottom of Pyramid and Walker Basins lie at different elevations. The dashed line at 1310 m indicates the level of the highest sill in the Lahontan Basin system. When the water elevation reaches this level the nine individual lakes including Walker and Pyramid are connected.

3. Map showing areal extent of Lake Lahontan at its highest known level (∿1330 m) and areal exent of glaciers in Sierra Nevada. Solid areas include existing lakes.

4. Climatic parameter distributions used in evaporation rate simulations. Curves labeled Reno 1950-1975 show mean monthly observations taken at the Reno weather station. Curves with filled triangles and circles in Figure 4a indicate July-scaled decreases in temperature of 10 to 15°K, respectively. The curve with open squares indicates a temperature distribution decrease of 10°K throughout the year. In Figure 4b the curves with open circles and triangles indicate July-scaled decreases in precipitable water aloft (W) of 20 and 40%, respectively. The curve having filled circles indicates a distribution in which W was decreased 20% throughout the year. In Figure 4c curves having open squares and triangles indicate July-scaled increases in sky cover of 10 and 20%, respectively. The curve with filled circles indicates a distribution in which sky cover was increased by 10% throughout the entire year.

5. Results of evaporation rate simulations. T_a refers to air temperature change relative to present-day value; (J) refers to July-scaled reduction in parameter, χ refers to percent increase in sky cover.

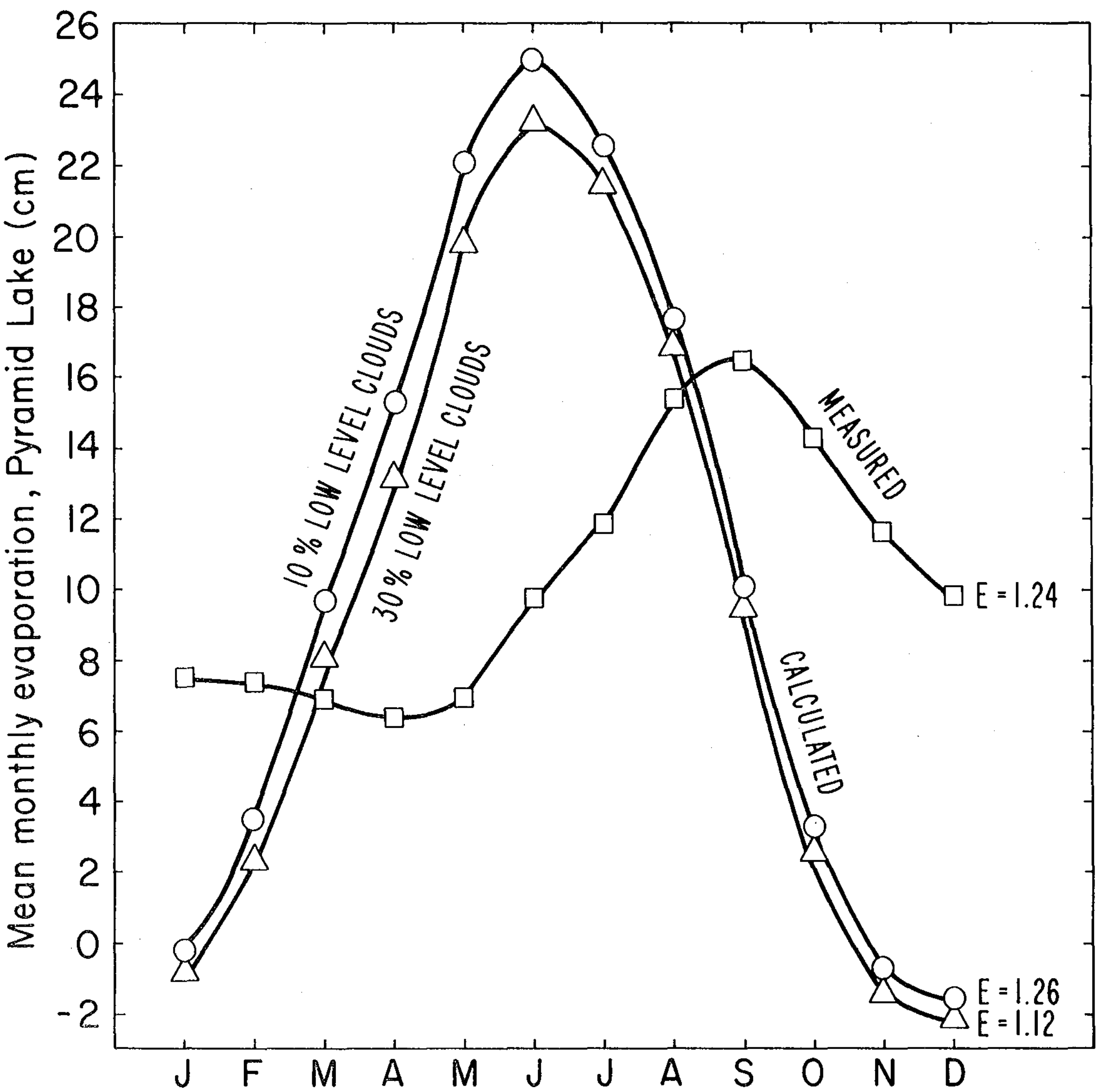

XBL 807-7253

FIGURE 1

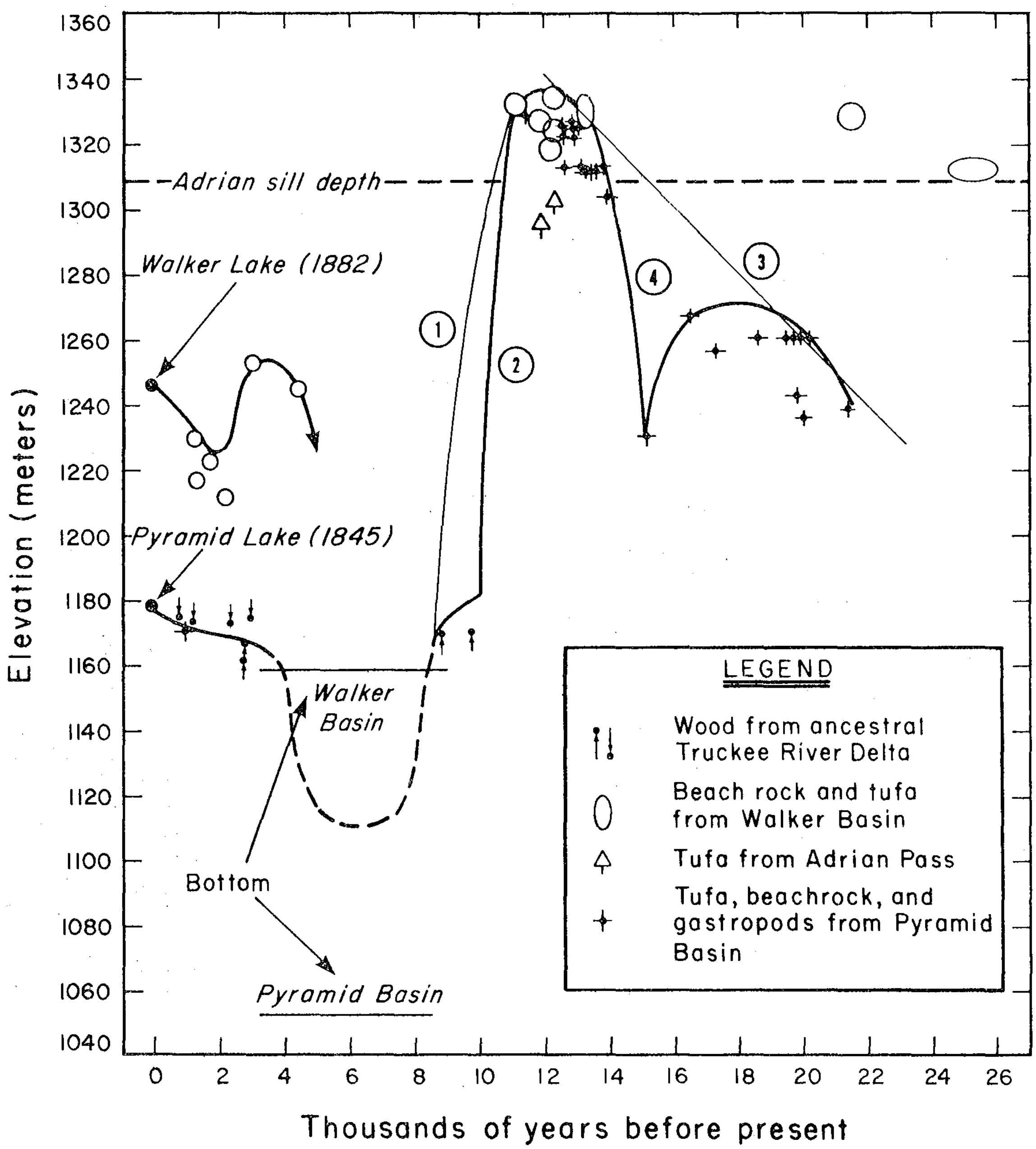

XBL 7911-13272

FIGURE 2

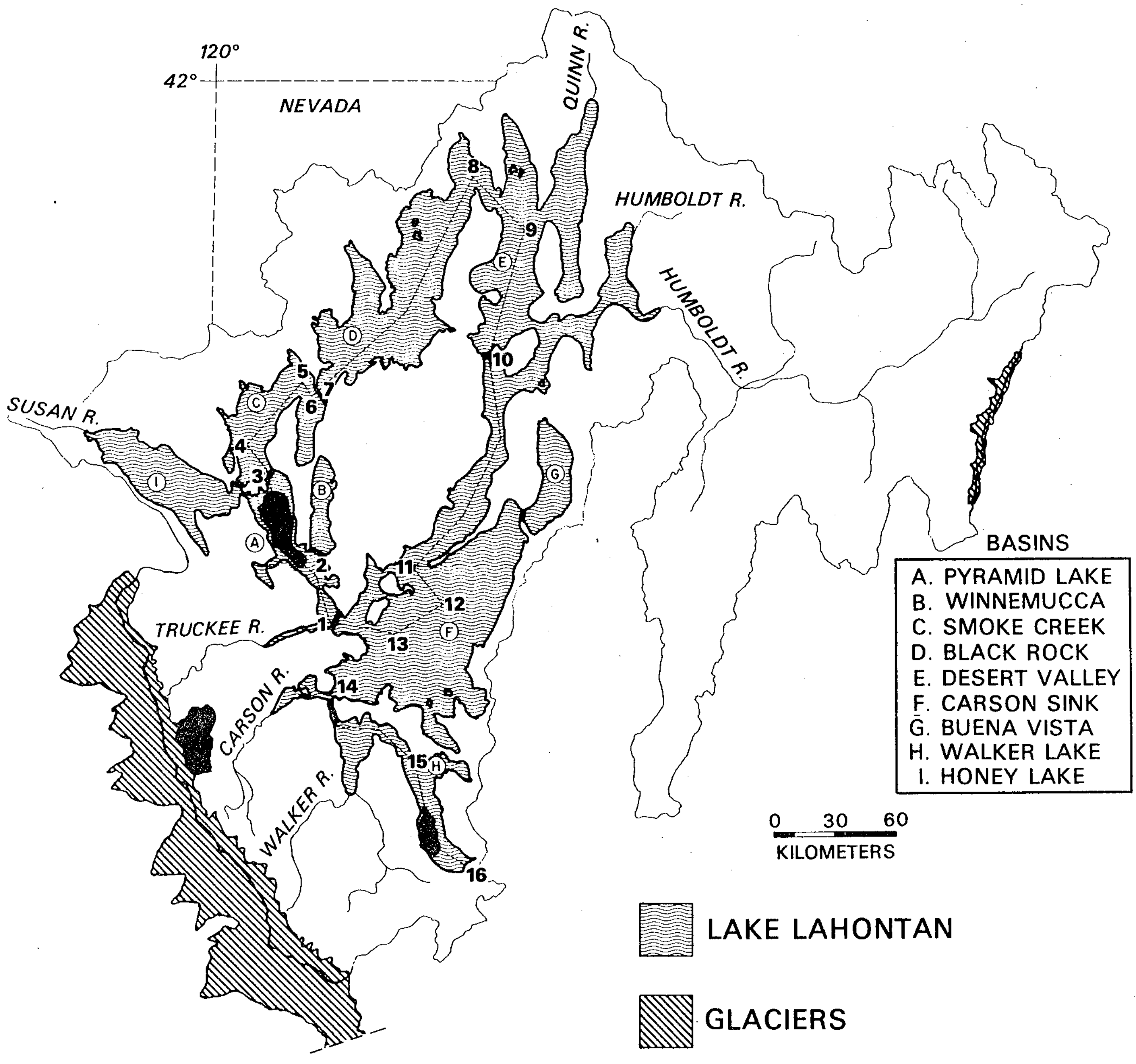

XBL 7712-11130A

FIGURE 3

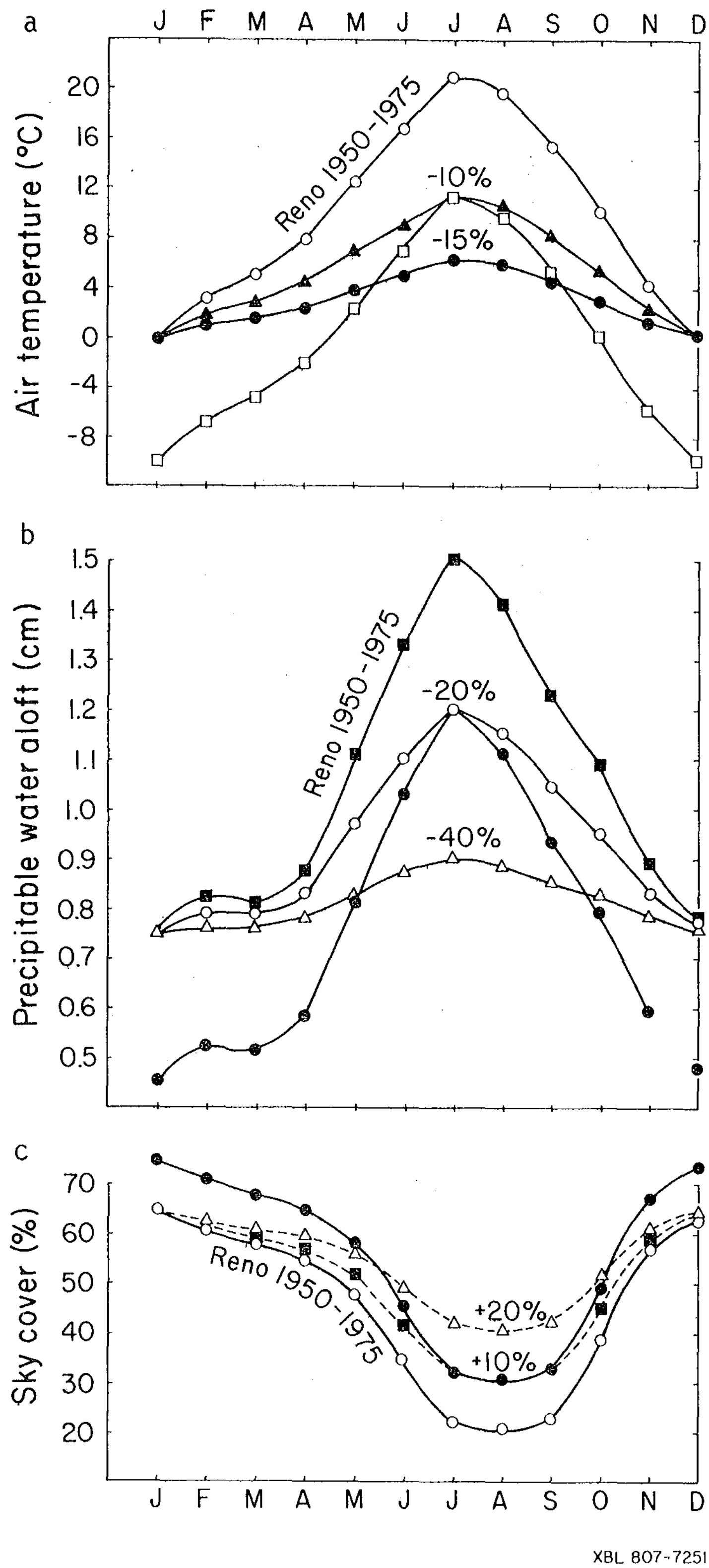
a
J F M A M J J A S O N D
Air temperature (°C)
20 16 12 8 4 0 -4 -8
Reno 1950-1975
-10%
-15%
b
Precipitable water aloft (cm)
1.5 1.4 1.3 1.2 1.1 1.0 0.9 0.8 0.7 0.6 0.5
Reno 1950-1975
-20%
-40%
c
Sky cover (%)
70 60 50 40 30 20
Reno 1950-1975
+20%
+10%
J F M A M J J A S O N D
XBL 807-7251

FIGURE 4

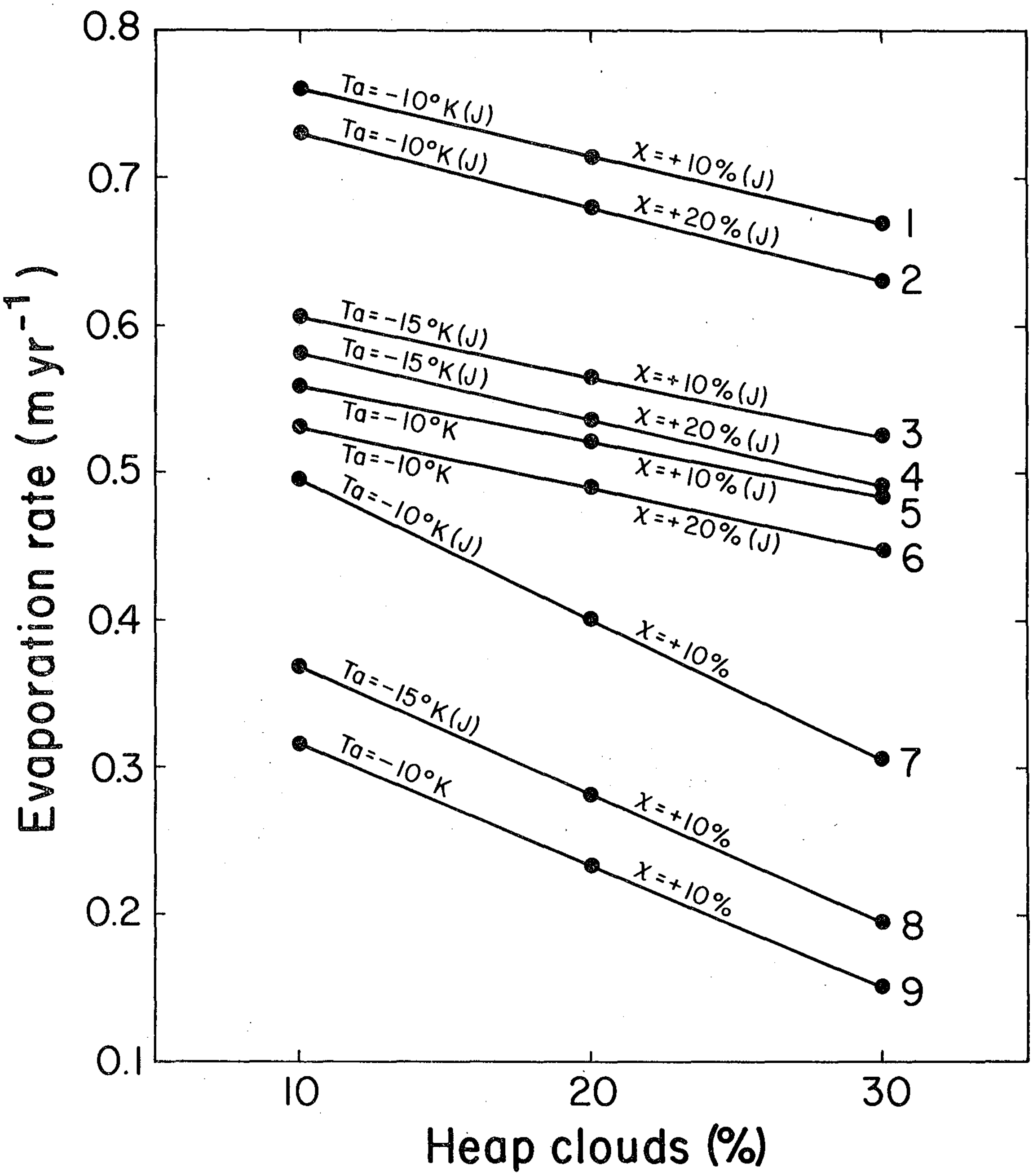

XBL 807-7252

FIGURE 5

This report was done with support from the United States Energy Research and Development Administration. Any conclusions or opinions expressed in this report represent solely those of the author(s) and not necessarily those of The Regents of the University of California, the Lawrence Berkeley Laboratory or the United States Energy Research and Development Administration.